
Title: Highly selective and direct oxidation of cyclohexane to cyclohexanone over vanadium exchanged NaY at room temperature under solvent-free conditions

Author: Nabanita Pal Malay Pramanik Asim Bhaumik Mahammad Ali

PII: S1381-1169(14)00234-9
DOI: http://dx.doi.org/doi:10.1016/j.molcata.2014.05.027
Reference: MOLCAA 9127

To appear in: *Journal of Molecular Catalysis A: Chemical*

Received date: 17-3-2014
Revised date: 26-5-2014
Accepted date: 27-5-2014

Please cite this article as: N. Pal, M. Pramanik, A. Bhaumik, M. Ali, Highly selective and direct oxidation of cyclohexane to cyclohexanone over vanadium exchanged NaY at room temperature under solvent-free conditions, *Journal of Molecular Catalysis A: Chemical* (2014), http://dx.doi.org/10.1016/j.molcata.2014.05.027

## Graphical Abstract

# Highly selective and direct oxidation of cyclohexane to cyclohexanone over vanadium exchanged NaY at room temperature under solvent-free conditions

Nabanita Pal,[a] Malay Pramanik,[b] Asim Bhaumik*[b] and Mahammad Ali*[a]

[a] *Department of Chemistry, Jadavpur University, Kolkata 700 032, India.*

[b] *Department of Materials Science, Indian Association for the Cultivation of Science, Jadavpur, Kolkata, 700 032, India.*

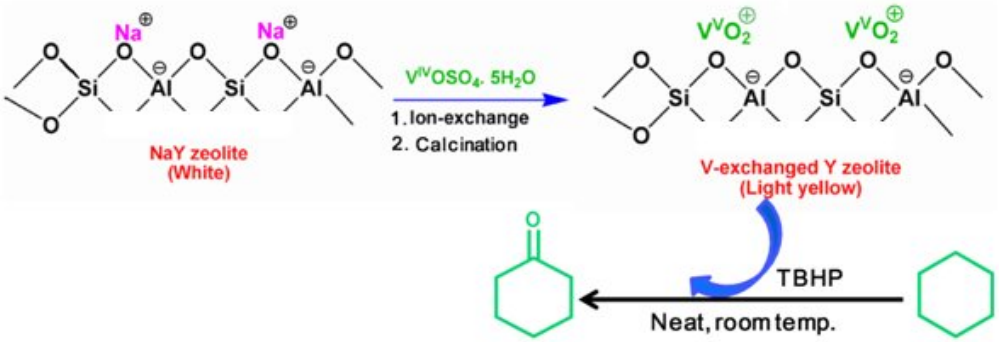


$VO_2^+$ exchanged Y zeolite has been synthesized by ion exchange over NaY zeolite with $VOSO_4$ under aqueous medium in open air. The material shows extraordinary efficiency for the solvent-free highly selective direct oxidation of cyclohexane to cyclohexanone at room temperature.

## Research Highlights

- Vanadium exchanged zeolite Y synthesized through simple ion-exchange.
- One step highly selective oxidation of cyclohexane to cyclohexanone
- High selectivity of cyclohexanone catalyzed by V-Y in the presence of TBHP oxidant.
- Reaction proceeds over V-Y under solvent-free condition at room temperature.

# Highly selective and direct oxidation of cyclohexane to cyclohexanone over vanadium exchanged NaY at room temperature under solvent-free conditions

Nabanita Pal,[a] Malay Pramanik,[b] Asim Bhaumik*[b] and Mahammad Ali*[a]

[a] *Department of Chemistry, Jadavpur University, Kolkata 700 032, India.*

[b] *Department of Materials Science, Indian Association for the Cultivation of Science, Jadavpur, Kolkata, 700 032, India.*

* Corresponding authors.

E-mail: msab@iacs.res.in (A. Bhaumik)

mali@chemistry.jdvu.ac.in (M. Ali).

**Abstract**

Vanadium exchanged zeolite Y has been synthesized by simple ion-exchange on NaY and resulting V-Y material has been employed as a heterogeneous catalyst for highly selective and direct one-pot liquid phase oxidation of cyclohexane to cyclohexanone under solvent-free conditions at room temperature. The catalyst (V-Y) has been thoroughly characterized by powder X-ray diffraction (PXRD), $N_2$ sorption, transmission electron microscopic (TEM), Fourier transform infrared (FT IR), UV-visible, X-ray photoelectron spectroscopic (XPS) and atomic absorption spectroscopic (AAS) analyses. The selective oxidation reaction proceeds smoothly over this V-containing heterogeneous catalyst in the presence of *tert*-butylhydroperoxide (TBHP) as oxidant and the progress of the reaction has been monitored thoroughly by gas chromatographic (GC) and gas chromatography coupled with mass spectrometric (GC-MS) analyses. The recycling efficiency of the V-Y catalyst has been tested by conducting the catalytic reaction repeatedly with the recovered catalyst, where almost retention of the original catalytic activity and selectivity after five reaction cycles has been observed. The effect of oxidant amounts on the catalytic reaction has been studied. Mechanistic pathway for the catalytic reaction over this inexpensive, non-air sensitive, eco-friendly and reusable vanadium exchanged zeolite has been proposed, suggesting future potential of V-Y in solvent-free liquid phase selective oxidation reactions under very mild reaction conditions.

*Keywords:* Cyclohexane oxidation, cyclohexanone, NaY zeolite, ion-exchanged Y, liquid phase oxidation, solvent-free conditions.

**Introduction**

Saturated hydrocarbons like *n*-hexane, cyclohexane etc. can be catalytically converted to a mixture of aliphatic and aromatic fine chemicals through a wide variety of chemical reactions [1], but it's very challenging to oxidize them selectively into a value added chemicals in a controlled fashion under mild reaction conditions [2-4]. Selective liquid phase oxidation of cyclohexane to cyclohexanone via activation of relatively inert C-H bond is a very important reaction in chemical industry. Because, a great majority of cyclohexanone combined with cyclohexanol (a mixture called 'KA oil', K= ketone, A= alcohol) is consumed for synthesis of ε-caprolactam and the remaining portion is supplied for the preparation of adipic acid, both of which are employed as important precursors for the manufacturing nylon 6 and nylon 6,6 polymers [5]. Conventionally, cyclohexanone is produced in homogeneous medium from the aerobic oxidation of cyclohexane at elevated temperature (423-433 K) and high pressure (1-2 MPa) using cobalt or metal-boric acid catalysts [6]. But this process suffers from the disadvantages like low conversion, poor selectivity towards main products, catalyst separation and environmental hazards [7]. Reactions carried out in heterogeneous media in the presence of Co, Fe-based catalysts give lower yield of the main products or require involvement of toxic solvents [8], which are environmentally not acceptable.

In recent times a wide range of catalytic processes have been developed globally for the environment benign green synthesis of cyclohexanone over different heterogeneous catalysts [9,10]. A solvent-free high temperature oxidation of cyclohexane using 1.0 MPa $O_2$ pressure over transition metal containing ZSM-5 catalyst has been reported by Yuan et al., where the total conversion does not exceed 10 mol% even after using *tert*-butylhydroperoxide (TBHP) as initiator [11]. Similar attempts have also been made using Au/MgO [12], Cu-supported SBA-15 [13], gold C-scorpionate complexes [14], Au nanoparticle supported silica [15], Ce/AlPO-5 [16],

Bi-SBA-15 [17], etc. in the presence of peroxides or under $O_2$ pressure for selective oxidation of cyclohexane. Hattori et al. have reported a green pathway for cyclohexane oxidation via photo-induced reaction over reactive $Fe/TiO_2$ catalyst [10]. Similarly, Shiraishi et al have reported the photocatalytic oxidation of cyclohexane with molecular oxygen over $WO_3$ loaded with Pt nanoparticles under irradiation of visible light, which leads to mixture of cyclohexananol and cyclohexanone [18]. However, most of these methods neither require high temperature nor bear a significantly low conversion level of cyclohexane. In this context, remarkably high catalytic conversion (>80%) of cyclohexane together with high selectivity for ketone product has been observed by Sarkar et al. who have performed the reaction at room temperature using Cu nanocluster supported over $Cr_2O_3$ [19]. But they could not avoid considerable amount of cyclohexanol along with the main ketone product and involvement of organic solvent in this partial oxidation reaction. On the other hand, we have observed high selectivity for cyclohexanol in the catalytic oxidation of cyclohexane over Cr-MCM-41 under liquid phase reaction conditions using TBHP as oxidant [20]. Hence, a suitable environment friendly microporous/mesoporous catalyst is very demanding, which can work efficiently under solvent-free conditions in the selective catalytic transformation of cyclohexane to cyclohexanone at room temperature.

Microporous zeolites, which bear cation exchange sites in the crystalline alumnosilicate frameworks can be the ideal host to carry out liquid phase catalytic reactions under environment friendly conditions [21-24]. Thus, keeping all these developments in mind we have synthesized vanadium exchanged NaY zeolite material, which could act as an efficient catalyst for the liquid phase oxidation reactions under very mild conditions. There are number of successful reports on liquid phase oxidation of cyclohexane over V-based catalysts, which require relatively severe

reaction conditions [25]. Due to high oxidizing property of 3*d* transition elements, when they are loaded in the aluminosilicate framework of NaY zeolites they can often employed in the liquid phase oxidation reaction [26]. V-containing materials especially showed excellent catalytic properties for various critical oxidation reactions, like hydroxylation of benzene to phenol [27], functionalization of *n*-butane to maleic anhydride [28], etc. Zeolitic framework being highly stable, inexpensive, non-corrosive, environment friendly and have inherent ability for high product selectivity could be employed as good support for different heteroelements [29,30]. Thus, when the vanadyl cation has been exchanged for Na in NaY the resulting material can serve as efficient heterogeneous catalyst for hydrocarbon oxidation with very high K/A ratio. Herein, we report a very simple, environment friendly, highly selective and one-pot route for the oxidation of cyclohexane to cyclohexanone over V-Y zeolite. In addition, investigations have been carried out to understand the role of oxidant, catalyst amounts and porous solid supports for this highly selective conversion of cyclohexane to cyclohexanone. Further attempts are also made to test the recyclability of the catalyst and to check the probability of the leaching of $VO_2^+$-species from the catalyst surface.

**Experimental section**

**Materials used.** NaY zeolite and $VOSO_4.5H_2O$ used for preparation of the catalyst were purchased from Sigma-Aldrich and Loba Chemie (India), respectively. Cyclohexane (Sigma-Aldrich) and TBHP (5.0-6.0 M in decane, Sigma-Aldrich) were used as substrate and oxidizing agent, respectively. All the chemicals were used without further purification.

**Catalyst synthesis.** $VO_2^+$-exchanged NaY zeolite (designated as V-Y) was prepared exchanging the $Na^+$ ions of NaY by V(IV) ions via aqueous ion-exchange method followed by calcination in air. First, NaY was activated by heating at 773 K in air for 6 h. In a typical synthesis, 10.0 mmol

of $VOSO_4.5H_2O$ was dissolved in 30 ml of distilled water followed by addition of 1.0 g activated NaY. Then this mixture was stirred at 363 K for 24 h during which the color of the mixture changed from blue to deep green. Then the reaction mixture was cooled to room temperature, filtered and washed thoroughly with hot distilled water till the filtrate became colorless. This ion-exchange process was repeated twice more to get higher loading of vanadium into zeolite Y. The material thus obtained was dried at 373 K in air for overnight and finally heated at 773 K for about 4 h to get yellow vanadium-exchanged material V-Y. A simple schematic representation of formation of V-Y catalyst is shown in Scheme 1.

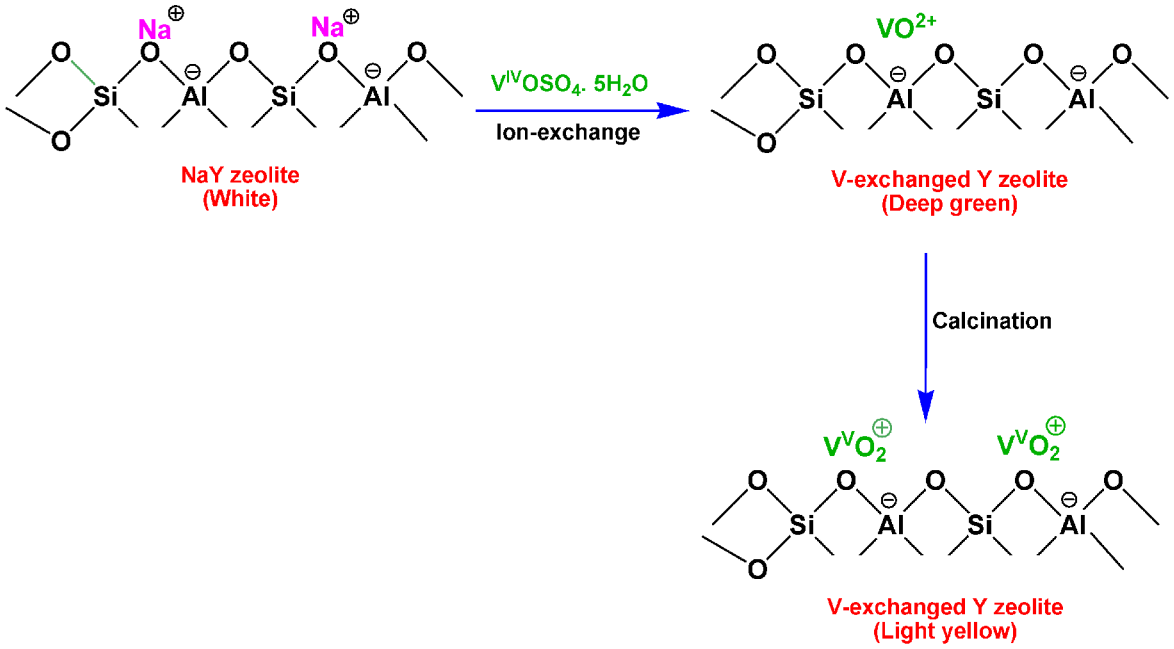


**Scheme 1:** Schematic representation depicting the formation of V-exchanged Y zeolite (V-Y).

**Physicochemical characterizations.** Powder X-ray diffraction (PXRD) patterns of the vanadium exchanged NaY zeolite as well as NaY were recorded by a Bruker AXS D-8 Advance diffractometer operated at 40 kV voltage and 40 mA current, calibrated with a standard silicon sample using Ni-filtered Cu-$K_\alpha$ ($\lambda$ = 0.15406 nm) radiation. The diffraction data was collected in

a $2\theta$ range of 5-$60^0$ with scan rate and step size of $0.1^0$ $s^{-1}$ and $0.02^0$ $step^{-1}$, respectively. BET surface areas of the parent zeolite and V-exchanged samples were measured from nitrogen adsorption/desorption isotherms obtained by using a Quantachrome Autosorb 1C instrument at 77 K temperature. Prior to gas adsorption, the sample was degassed for 5 h at 413 K. Total pore volume was estimated from the $N_2$ uptake at the relative pressure of $P/P_0 = 0.99$. UV–visible diffuse reflectance spectra (DRS) were obtained by using a Shimadzu UV 2401PC spectrophotometer with an integrating sphere attachment; a $BaSO_4$ pellet was used as background standard and analysis was done with solid sample in the wavelength range of 200-800 nm at room temperature (303 K). A Perkin-Elmer 3100 atomic absorption spectrometer was used to measure the percentage of vanadium in our catalyst. For this chemical analysis the material was digested with $H_2SO_4$, HF and few drops of $H_2O_2$ and then dissolved in water to prepare an aqueous solution of V-Y. Fourier transform infrared (FT IR) spectra of the samples were recorded at room temperature on KBr pellets by using a Perkin Elmer Spectrum BX FT IR spectrophotometer. X-ray photoelectron spectroscopic (XPS) analysis of V-Y was performed on an Omicron nanotech system operated at 15 kV and 20 mA with a monochromatic Al-$K_\alpha$ (1486.6 eV) X-ray source. Prior to the analysis, the powder sample was dispersed in ethanol for 30 min under sonication and a thin film was prepared by spin coating method. The thin film was heated at 393 K under vacuum for 4 h before transferring it into the XPS instrument.

**Oxidation of cyclohexane.** A mixture of cyclohexane (1.0 mmol) and 0.75 g of TBHP (in decane) was taken in a 25 mL round bottomed flask. Then 0.05 g of pre-activated catalyst heated at 423 K for 2 h was poured into the mixture. The mouth of the flask was closed with glass stopper and Teflon tape. Then the mixture was stirred vigorously through a magnetic stirrer at 303 K for definite period of time. Progress of the reaction has been monitored by withdrawing

aliquots from the reaction mixture at regular intervals and analyzing with help of an Agilent 7890A gas chromatograph (FID detector) fitted with a capillary column. The products were identified using known standards and also by using a Perkin Elmer Clarus 680 gas chromatograph attached with Clarus SQ 8 T mass spectrometer (GC/MS) which records mass spectra of the sample in $EI^+$ mode.

**Results and Discussion**

**PXRD analysis.** In Figure 1 the powder XRD patterns of pure NaY and vanadium exchanged V-Y are shown. Diffraction peaks for NaY showed at $2\theta$ values of $6.18^0$, $10.13^0$, $11.96^0$, $15.64^0$, $20.30^0$, $23.70^0$, $27.02^0$, $31.30^0$, $34.14^0$, which represent the characteristic reflection planes for (111), (220), (311), (331), (511), (440), (533), (642), (555) and (666), respectively of typical

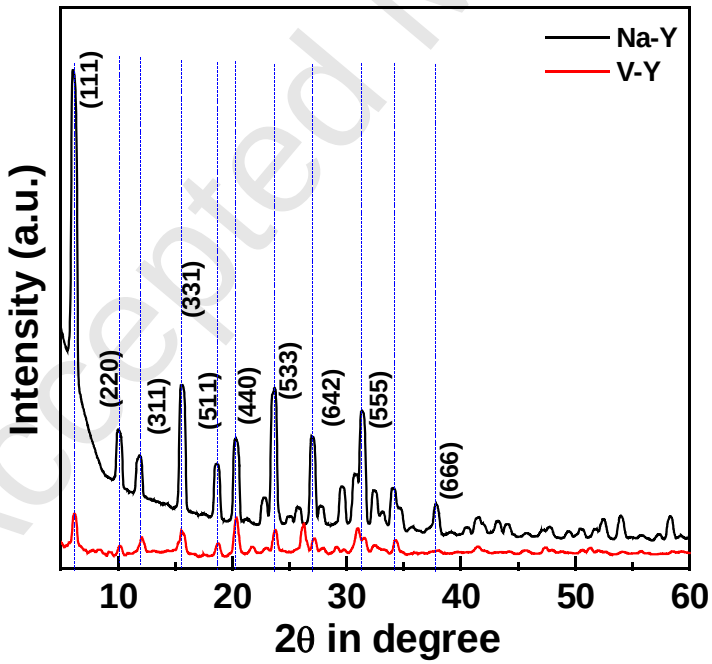


**Figure 1.** Powder XRD patterns of (a) Na-Y and (b) V-Y samples. Vertical lines indicate the peak positions in both the samples.

NaY zeolite [31]. The PXRD of V-Y exhibits an essentially similar pattern suggesting that the regularity of crystal structure of NaY zeolite is maintained in V-Y after the introduction of vanadium at the exchange sites. However, a little change in relative intensities of the peaks upon exchange with $VO_2^+$ species in the zeolite cages is observed. The high loading of vanadium via systematic replacement of randomly distributed extra framework $Na^+$ ions in the zeolite causes the decrease in peak intensity of V-Y with respect to YZ sample [32]. The cell parameters ($a_{533}$) for NaY and V-Y calculated ($a_{hkl}$= $\{(d_{hkl})^2 \times (h^2 + k^2 + l^2)\}^{1/2}$) are 2.4608 nm and 2.4567 nm, respectively. Very little deviation in cell parameter of NaY zeolite suggested that metal exchange occurs at the extra framework sites.

**Porosity and BET surface area.** The porosity and related surface properties of NaY zeolite and vanadium exchanged V-Y materials have been obtained from the $N_2$ adsorption/desorption analysis at 77 K and respective isotherms are shown in Figure 2A. The BET surface area,

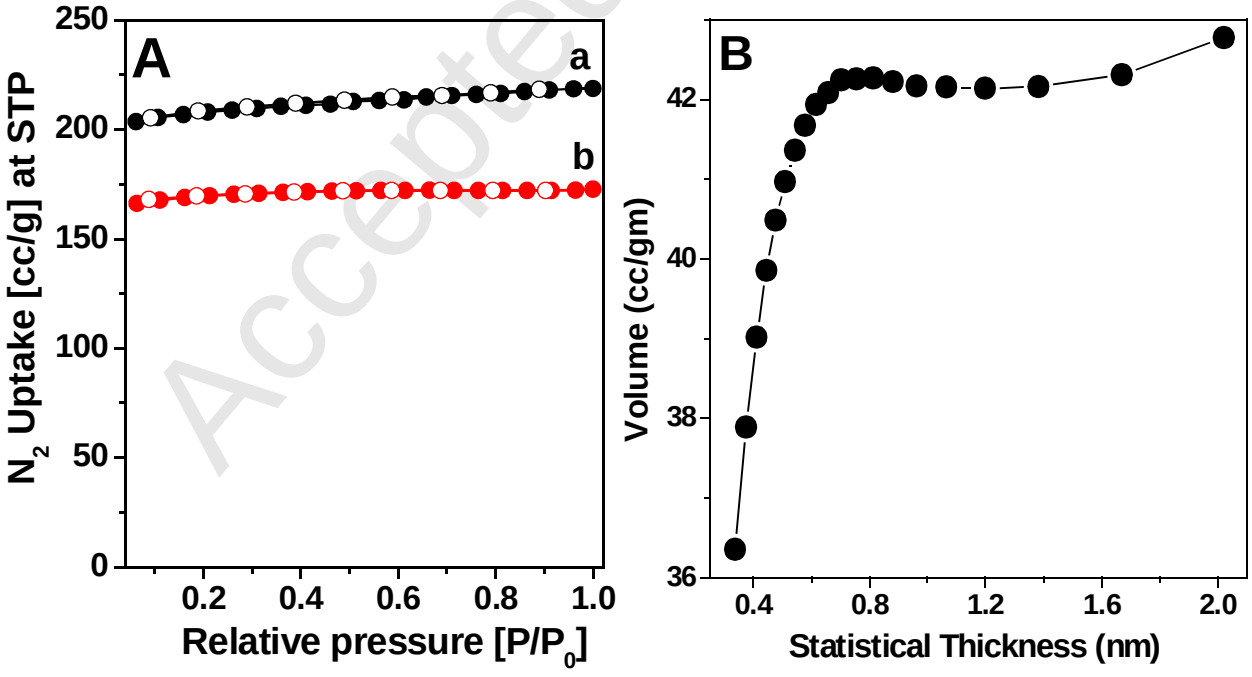

**Figure 2.** A: $N_2$ adsorption (●)-desorption (○) isotherms of the parent zeolite Na-Y (a) and V-Y (b) material. For clarity, Y-axis points of V-Y sorption have been 130. B: Adsorbed $N_2$ gas volume Vs statistical thickness of pores in the material.

**Table 1.** Physico-chemical data of the catalyst V-Y.

| Sample name | $S_{BET}$ [$m^2g^{-1}$] | $S_{micro}$ [$m^2g^{-1}$] | $S_{ext}$ [$m^2g^{-1}$] | $D_p$ [nm] | $V_t$ [$cm^3g^{-1}$] | $V_{micro}$ [$cm^3g^{-1}$] | Presence of V (%)[1] |
|---|---|---|---|---|---|---|---|
| Na-Y | 686 | 672 | 14.4 | 2.25 | 0.34 | 0.32 | - |
| V-Y | 139.4 | 135.0 | 3.80 | 2.59 | 0.063 | 0.060 | 15.10 |

$S_{BET}$ = BET surface area, $S_{micro}$ = micropore surface area, $S_{micro}$ = external surface area, $D_p$ = average pore diameter corresponding to the maximum of PSD curve, $V_t$ = total pore volume, $V_{micro}$ = micropore volume.

micropore surface area, external surface area, average pore diameter, total pore volume and micropore volume estimated from this surface analysis are summarized in Table 1. The sorption isotherm followed typical type I isotherm, characteristic of microporous materials [33]. Here, in case of V-Y material nitrogen uptake takes place in a large amount at very low relative pressure $P/P_0$ of $N_2$ corresponding to the filling of micropores [34]. But after monolayer adsorption at low $P/P_0$ range $N_2$ uptake is almost constant and no hysteresis is found in the region of higher relative pressure, indicating the absence of mesopores or interparticle porosity in V-Y. BET surface area of V-Y is 139 $m^2g^{-1}$, which is decreased sharply with respect to that of pure NaY zeolite (686 $m^2g^{-1}$). This could be attributed to the decrease of crystallinity in the V-exchanged sample as noticed from the PXRD pattern (Figure 1) as well as high loading of $VO_2^+$ species having high molar mass vis-à-vis $Na^+$. The *t*-method micropore analysis revealed that the material is consisting of internal micropore area of 135.2 $m^2g^{-1}$ together with external mesopore area of 3.8

$m^2g^{-1}$. The corresponding micropore volume is 0.06 $ccg^{-1}$. The graphical plot of adsorbed gas volume with respect to the statistical thickness obtained from sorption analysis is shown in Figure 2B. From this figure it is clear that the maximum volume of the adsorbed gas ($N_2$) has been occupied at the micropores of V-Y.

**Electron microscopic analysis**. In order to investigate the nanoscale structural features of the sample the HR TEM analysis of V-Y has been carried out and the results are shown in Figure 3. High resolution image of NaY specimen is shown in Figure 3A, where micropores of sub-

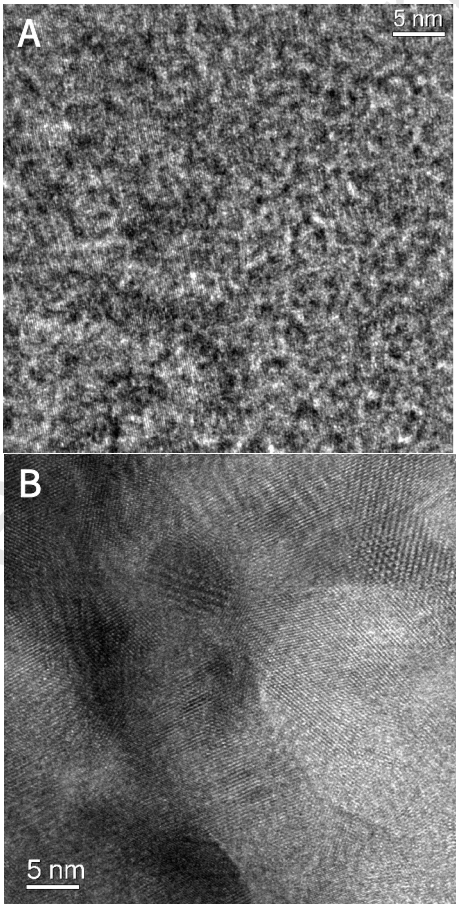


**Figure 3.** A: TEM image of the sample V-Y and B: TEM image of the sample showing reflection planes.

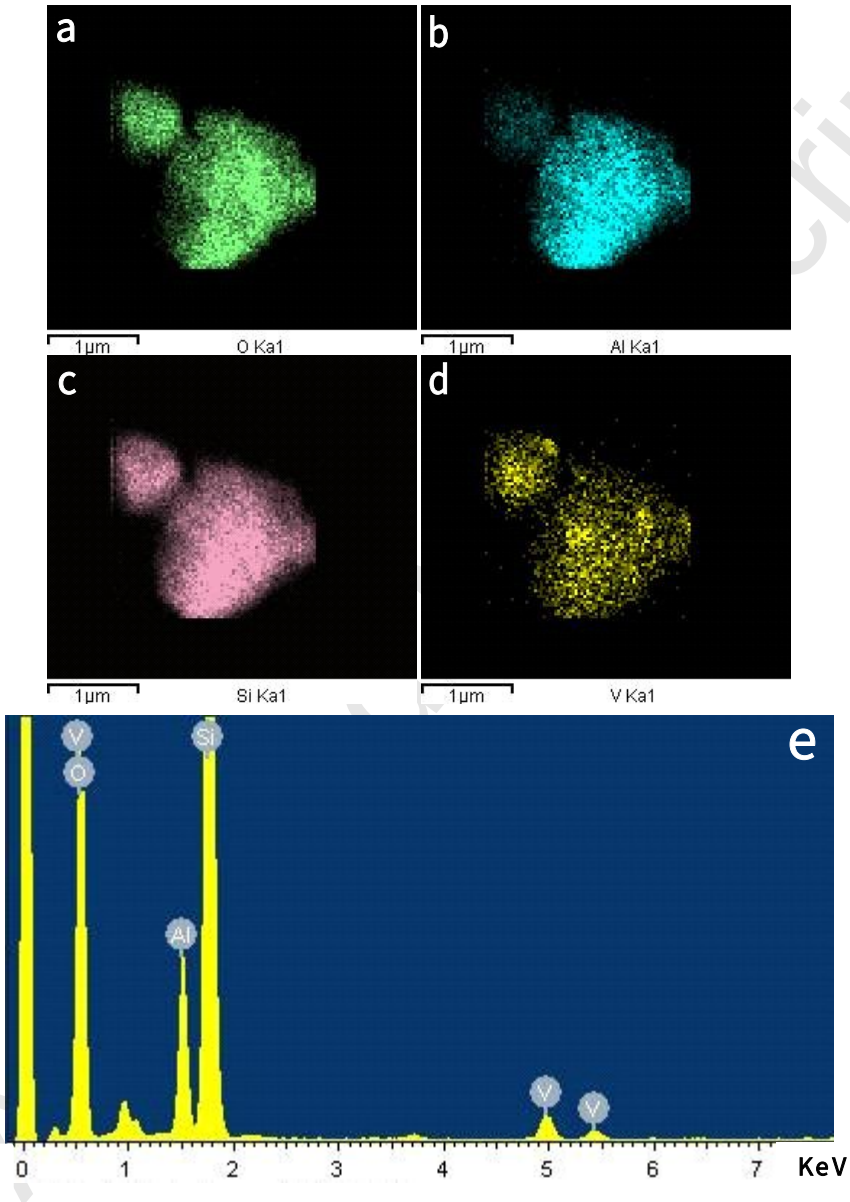


**Figure 4.** EDS elemental mapping of V-Y sample. a: O, b: Al, c: Si and d: V elements, respectively. e: the whole EDX spectrum of the sample V-Y.

nanometer scale is observed all over the sample. On the other hand crystalline well-resolved lattice planes of vanadium exchanged Y is observed in the Figure 3B. A little perturbation

observed in the image is due to the presence of magnetic V species in the sample. From the EDS elemental mapping (Figure 4) the homogeneous distribution of all the elements, mainly distribution of V throughout the framework of the material is clearly observed. The EDS spectrum shown in Figure 4e indicates that all the Na ions of NaY zeolite have been successfully exchanged during ion-exchange method by V ion.

**FT IR spectroscopic data.** Information about framework vibrations as well as bonding/ connectivity in NaY and V-Y samples could be obtained from the FT IR analysis. FT IR spectra of both Y zeolites are shown in Figure 5. A broad absorption band in the range of 2900-3600 $cm^{-1}$ and a sharp peak near 1630 $cm^{-1}$ which could be attributed to the O-H stretching frequency

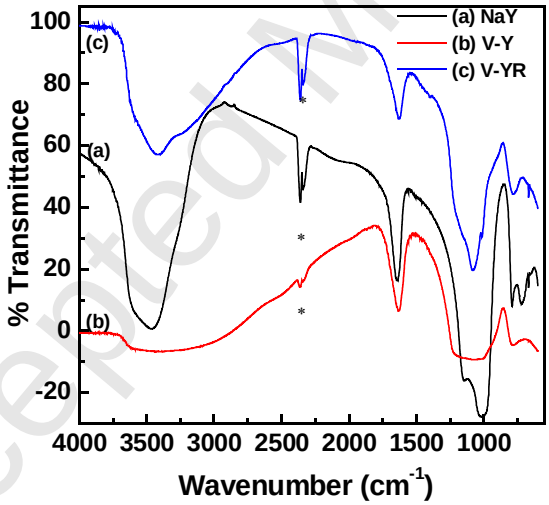


**Figure 5.** FT IR data of (a) Na-Y, (b) the catalyst V-Y and (c) the recovered catalyst V-YR. (*) indicates the peak for $CO_2$.

of the physisorbed water molecules [28]. The broad and strong band near 1000 $cm^{-1}$ could be attributed to the asymmetric stretching vibration of $(Si/Al)O_4$ units of zeolite framework [35]. The other peaks at *ca.* 1150 and 790 $cm^{-1}$ are also characteristic of typical zeolite structure [36].

Almost no shift in the absorption peaks in the case of V-Y with respect to NaY is observed, clearly suggesting that zeolite framework is remained intact upon the loading of the vanadium ions. But the absorption band for V=O species cannot be traced in the region of ~1000 $cm^{-1}$ due to superimpose of this peak with a strong peak due to zeolite framework at this position [36].

**XPS analysis.** Additional confirmation of the chemical environment and the valence state of the vanadium ion in V-Y zeolite can be obtained from the electron spectroscopic analysis at the surface. Figure 6A-D exhibits high resolution core level X-ray photoelectron spectra of V 2p, Si

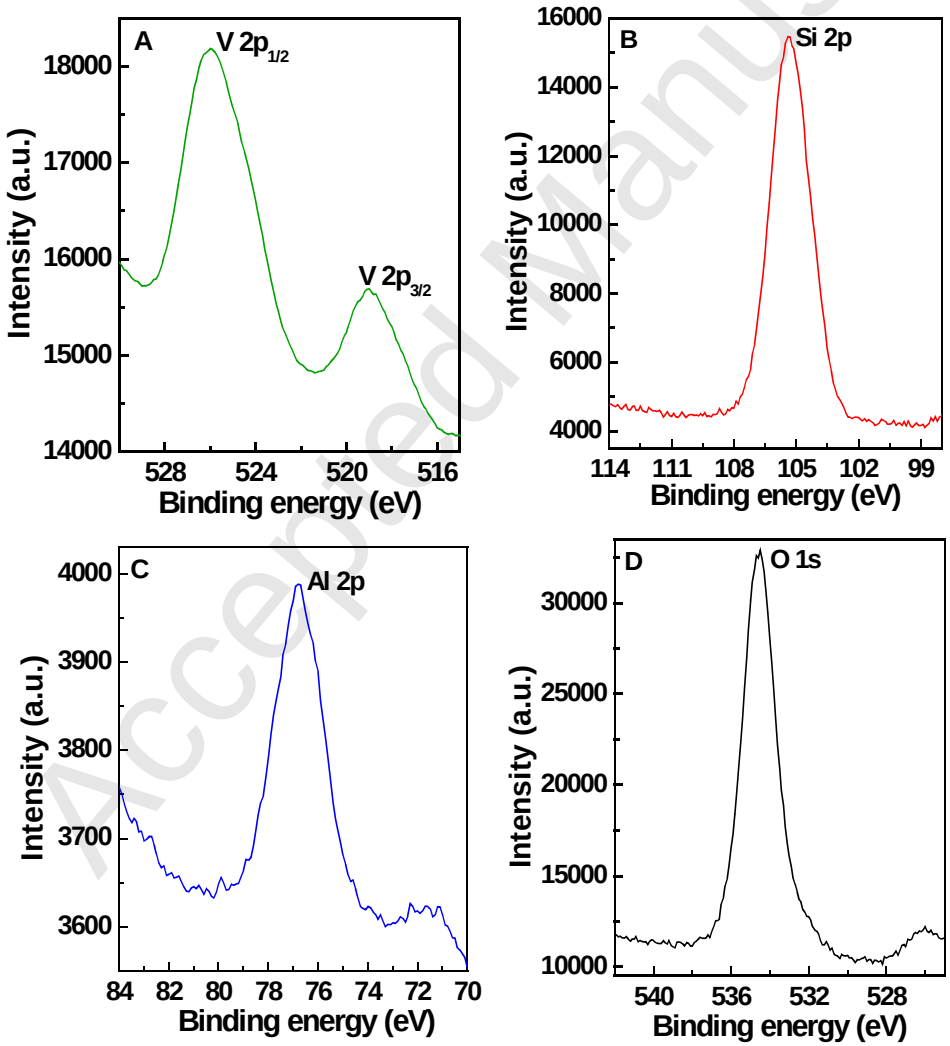


**Figure 6.** X-ray photoelectron spectra of A: V 2p, B: Si 2p, C: Al 2p and D: O 1s core level electrons of V-Y.

2p, Al 2p along with O 1s electrons of V-Y, respectively and the binding energy values in eV corresponding to the individual peak (after charge correction with reference to O 1s peak referenced at 532.0 eV) are presented in Table 2. High resolution V 2p spectrum consisting two peaks near 516.51 for V $2p_{3/2}$ and 523.42 eV for V $2p_{1/2}$ suggesting the presence of intra-zeolite V(V) oxide in the material [37,38]. This binding energy values suggest that V(IV) of vanadyl sulphate has been oxidized to V(V) during heating in air at temperature at 773 K. Besides Si 2p electron showing broad peak near 102.85 eV, Al 2p peak at 74.30 eV and O 1s peak at 532.0 eV strongly support the evidence for zeolite framework of the catalyst and these values matched quite well with the literature data of NaY [39]. The surface atomic composition of V-zeolite analyzed with the help of CasaXPS software showed Si:O:Al:V molar ratio of 4.0:11.73:1.70:1.0, suggesting the presence of exchanged V-sites almost at the quantitative level.

**Table 2.** Binding energies of core level electrons obtained from XPS study of V-Y zeolite (with reference to the O 1s binding energy at 532.0 eV)

| Core level electron | Binding energy (eV) |
|---|---|
| V 2p | 516.51<br>523.42 |
| Si 2p | 102.85 |
| Al 2p | 74.30 |
| O 1s | 532.00 |

**Cyclohexane oxidation.** In addition to the XPS analysis, we have carried out the AAS analysis for V-Y and the material showed a significantly large amount of V loading (~15%, Table 1). High V-loading has prompted us to explore the liquid phase catalytic oxidation of vanadium

exchanged NaY zeolite in the solvent-free selective oxidation of cyclohexane (CH) to cyclohexanone (CHone) using TBHP as oxidant. The conversions under different reaction conditions are calculated from gas chromatographic (GC) analysis and these are presented in Table 3. All catalytic experiments are carried out at room temperature (303 K). It is observed that V-Y showed a very large cyclohexane conversion (about 98%) together with 100% selectivity for cyclohexanone when the reaction was carried out at 303 K for 72 h (Entry 1). For convenience, we have monitored the progress of the reactions after 24 h intervals. Formation of

**Table 3.** Catalytic oxidation of cyclohexane (CH) to cyclohexanone (CHone) over different catalysts.

| Entry | Catalyst | Reaction time (h) | CH conversion (%) | CHone selectivity (%) |
|---|---|---|---|---|
| 1 | V-Y | 72 | 97.76 | 100 |
| 2 | V-Y | 24 | 38.10 | 100 |
| 3 | NaY | 24 | 3.23 | - |
| 4[a] | - | 24 | 1.81 | - |
| 5[b] | V-Y | 24 | 0.00 | - |
| 6[c] | V-Y | 24 | 2.36 | 100 |
| 7[d] | V-Y | 24 | 9.65 | 100 |

Conversion (%) = [Peak area of product obtained from GC/Summation of peak area of substrate and product obtained from GC]*100.

Reaction conditions: cyclohexane = 1 mmol, TBHP = 0.75 g, catalyst = 0.05 g, room temperature,

[a] blank reaction carried out without any catalyst.

[b] reaction carried out without TBHP.

[c] reaction carried out using $H_2O_2$ instead of TBHP.

[d] reaction carried out with 1:1 mixture of $H_2O_2$ and TBHP.

cyclohexanone as the only product with no other intermediate oxidation product like cyclohexanol and this is confirmed from the GC-MS (Figure S1) and the mass spectroscopic analysis (Figure S2). Blank reactions have been carried out without catalyst or TBHP (Entry 4 and 5) and they show almost no conversion, which implies that the oxidation reaction cannot proceed without the aid of either TBHP oxidant or V-catalyst alone. Pure NaY zeolite also failed to show any catalytic activity for the cyclohexane oxidation (Entry 3). We have carried out the reaction under other mild oxidant $H_2O_2$, (Entry 6) or with a mixture of $H_2O_2$ and TBHP (Entry 7). However, in both cases we could not get the desired yield of product cyclohexanone. These results suggested obvious catalytic role of vanadium species and TBHP as an efficient oxidant in this selective catalytic reaction.

The effect of changing reaction parameters like reaction time and the amount of TBHP on the selective oxidation of cyclohexane has also been examined. It is observed that, CHone formation is gradually increasing with reaction time, which is presented graphically in Figure 7A by % yield as against the reaction time in this plot. One of the reasons of linear increase of ketone percentage may be due to the direct conversion of CH to CHone during this reaction and thus no alcohol is detected as intermediate/side product. Effect of reaction time in the selectivity of cyclohexanone yield has already been mentioned in previous studies. On the other hand, the influence of oxidant amount on the cyclohexane conversion is also tested, which is displayed in Figure 7B. The plot shows a steep increase of CHone amount on changing the oxidant amount from 0.45 g to 0.75 g. But on further increase of the TBHP amount to 1.125 g the reaction rate did not follow the linear rise, which indicates that in the presence of large amount of oxidant a number of side products are formed and this caused a decrease in the actual yield of the desired product.

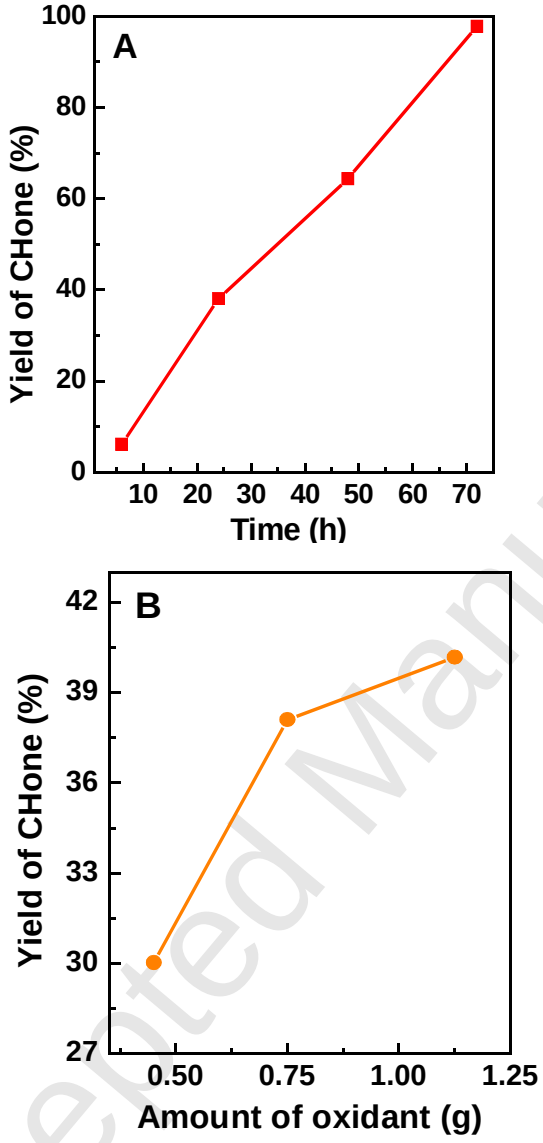


**Figure 7.** A: Effect of reaction time and B: the amount of TBHP on the % yield of cyclohexanone over V-Y catalyst.

Presence of electron-withdrawing counter ion (here oxo anion) [40], high loading of V or strong Lewis acidity of the oxo-metal catalyst ($V^{V}$=O) [41] as well as strong oxidizing potential of TBHP influence the product ratio of ketone to alcohol greatly in this cyclohexane oxidation reaction. 5.0-6.0 M solution of TBHP in organic solvent like nonane or decane is a comparatively strong and thermally stable oxidizing agent than conventional oxidant like $H_2O_2$,

containing large amount of active oxygen atoms [42,43]. TBHP being soluble in organic media can be readily activated by high-valent oxo-metal species and therefore it can be successfully used as oxidant in many selective oxidation reactions mediated by V-exchanged catalyst [43]. In the present case, a solvent-free complete organic mixture of TBHP/decane oxidant and cyclohexane along with $V^V$-exchanged Y zeolite could be responsible for the high selectivity of CHone formation. The catalytic activity of V-Y material has been compared to the other reported vanadium or oxovanadium species present in the solid heterogeneous supports (Table 4) [44-47]. Although, vanadium containing mesoporous materials showed good catalytic activity in this liquid phase cyclohexane oxidation, in all the cases mixture of cyclohexanol and cyclohexanone

**Table 4.** Comparative catalytic performance of reported oxidation catalysts with our materials.

| Entry | Catalyst | Time (h) | Temp (K) | Oxidant | Solvent | CH conversion (%) | CHone selectivity (%) | Ref. |
|---|---|---|---|---|---|---|---|---|
| 1 | V-MCM-41 | 12 | 373 | $H_2O_2$ | Acetic acid | 99.0 | 1.9 | 25 |
| 2 | V-HMS | 4 | 413 | $O_2$ | No solvent | 9.34 | 60.3 | 46 |
| 3 | VS-2 | 4 | 333 | $H_2O_2$ | Acetonitrile | 28[1] | - | 47 |
| 4 | $VOPO_4$ on alumina | 24 | 333 | $H_2O_2$ | Acetonitrile | 59.0 | 9.7 | 48 |
| 5 | V-MCM-41 | 12 | 373 | TBHP | Acetone or cyclohexane | 44.6 | 61.29 | 49 |
| 6 | V-MCM-41 | 12 | 373 | $H_2O_2$ | Acetone | 11.7 | 57.14 | 49 |
| 7 | V-Y | 72 | 303 | TBHP | No solvent | 97.7 | 100.0 | This work |

[1]TON = Turn over number, moles of cyclohexane converted per mole of V.

were main products together with low selectivity for cyclohexanone. As seen from the table that V-Y showed very high selectivity together with excellent conversion level under very mild

reaction conditions compared with other V-containing microporus and mesoporous supports. The high catalytic activity of V-Y zeolite together with excellent selectivity compared to mesoporous V-MCM-41 could be attributed to the fact that hydrophobic Y-zeolite surface facilitates stronger interaction with cyclohexane vis-à-vis hydrophilic MCM-41 support. Additionally high Brønsted acidity of Y zeolite over MCM-41 [50] could facilitate the protonation of the reaction intermediates. Under solvent-free conditions over V-Y the concentration of peroxide is much higher, which could help to proceed the reaction at relatively low temperature. Higher catalytic activity and enhanced selectivity of the zeolite surfaces over other molecular sieve supports and for the desired products is observed over other microporous materials also [51]

A mechanistic pathway for the one-pot oxidation of cyclohexane has been presented in Scheme 2. The reaction pathway for this direct-oxidation reaction in the presence of TBHP oxidant is supposed to proceed through free-radical chain reaction pathway as proposed by Nowotny et al [48]. The first step is the initiation step where $V^{V}$=O species react with TBHP to generate $^{t}BuOO^{\bullet}$ and $^{t}BuO^{\bullet}$ radical species. In propagation step these radicals abstract H atom from cyclohexane to generate highly reactive cyclohexyl ($C_6H_{11}^{\bullet}$) radical which readily converted to cyclohexyl peroxy radical ($C_6H_{11}$-$OO^{\bullet}$) on reaction with aerial oxygen dissolved in the medium. Cyclohexyl peroxy radical is the main propagator of this chain reaction. Since only ketone is our only final product instead of a mixture ketone and alcohol mixed Russell termination step is most likely to happen after propagation rather than normal termination [49]. So the reaction is terminated when two free radical $C_6H_{11}$-$OO^{\bullet}$ combines with $^{t}BuOO^{\bullet}$ to form cyclohexanone with release of one molecule oxygen and *tert*-butanol as byproduct (Scheme 2).

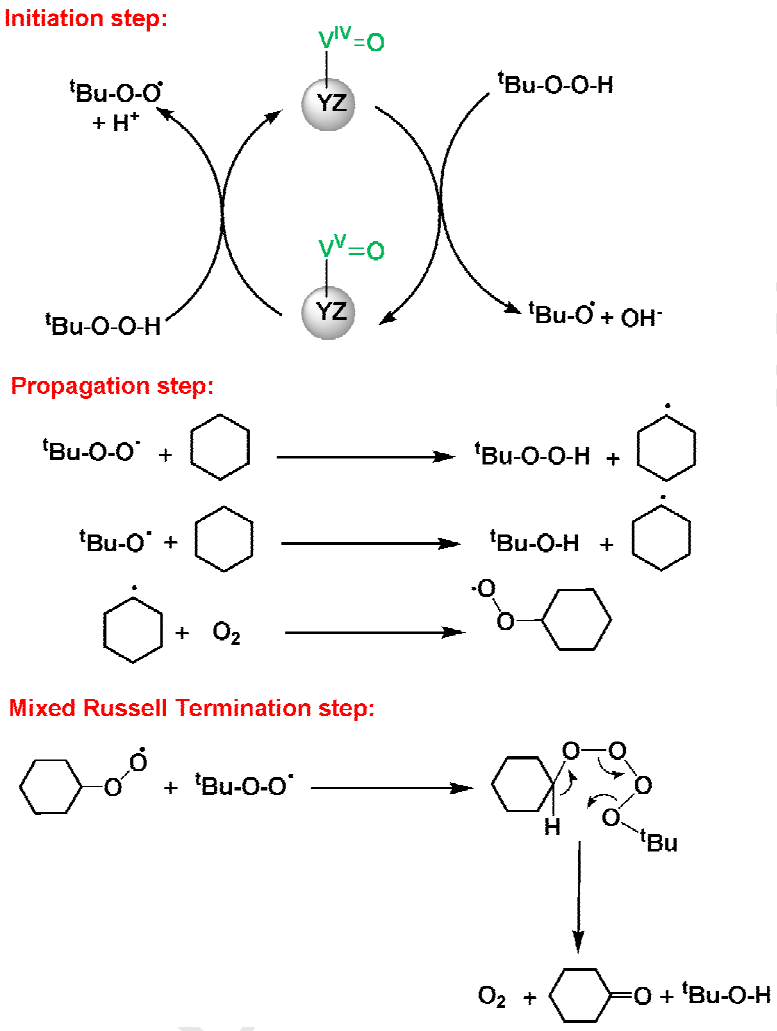


**Scheme 2:** Proposed mechanism for cyclohexane oxidation via free-radical reaction pathway over V-Y catalyst.

We have successfully employed the used V-Y catalyst for recycling experiments by simply recovering it from the reaction mixture through filtration followed by washing thoroughly with alcohol and acetone. The recovered catalyst has been dried and activated by heating at 773 K for 2 h for further use it the next cycle. FT IR spectrum of V-YR (Figure 5) shows that the recovered catalyst retains its framework and bonding with respect to the original one (V-Y). The

reusability test was performed with V-YR up to another four reaction cycle showing almost same extent (decrease of conversion after each cycle is < 2%) in cyclohexane conversion level (Figure 8) while maintaining exactly similar reaction conditions for each cycle. Little decrease in the conversion level is within the experimental error of GC analysis and could cause due to a very

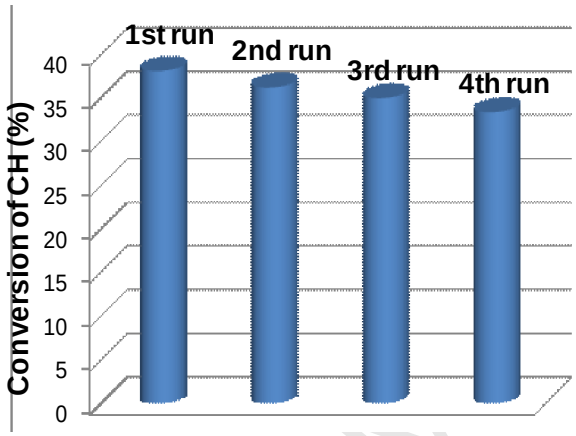


**Figure 8.** Recycling efficiency of V-Y in one pot oxidation of cyclohexane to cyclohexanone. For convenience all cycles are continued for 24 h only.

small amount of vanadium ion leaching. However, the V-Y catalyst does not lose its structural stability, which is indicated from the resemblance of its powder XRD and FT IR data with reference to that of the fresh one.[25] From this result it is evident that V-Y can act as an efficient heterogeneous catalyst for selective oxidation of cyclohexane with minimum leaching of $VO_2^+$ active species from the zeolite Y extraframework sites.

## Conclusions

A highly reactive V-Y zeolite bearing $VO_2^+$ at the exchange site of NaY zeolite has been synthesized through a simple ion-exchange method. V-Y showed excellent catalytic activity in highly selective one-pot oxidation of cyclohexane to cyclohexanone by using *tert*-

butylhydroperoxide as oxidant at room temperature. The reaction proceeds under solvent-free conditions, without any aid of toxic organic solvent and thus provide a very significant pollution-free route for the large scale production of cyclohexanone. The impact of catalytic reaction parameters and explanations of the highly selective one-pot synthesis of cyclohexanone are also discussed to get a clear overview in this eco-friendly oxidation reaction. High reactivity of V-Y under mild liquid phase oxidation reaction may motivate the researchers to explore its potential in other value added selective oxidation reactions.

**Acknowledgements**

NP is grateful to University Grants Commission (UGC), New Delhi for Dr. D. S. Kothari postdoctoral fellowship. MP thanks CSIR, New Delhi for a senior research fellowship. MA wishes to thank DST, New Delhi for providing research funding. MA and NP are thankful to Dr. T. K. Paine of Indian Association for the Cultivation of Science for providing GCMS facility in his laboratory. AB thanks DST, New Delhi for providing instrumental facilities through DST Unit on Nanoscience and DST-SERB project grants.

**References**

[1] N. M. Emanuel, E.T. Denisov, Z. K. Maizus, Liquid Phase Oxidation of Hydrocarbons, Plenum Press, New York, (1969).

[2] L. Que, W. B. Tolman, Nature 455 (2008) 333-340.

[3] T. Tatsumi, M. Nakamura, S. Negishi, H. Tominaga, J. Chem. Soc., Chem. Commun. (1990) 476-477.

[4] M. Nandi, P. Roy, A. Bhaumik, Dalton Trans. 40 (2011) 12510-12518.

[5] J. G. Speight, Chemical and Process Design Handbook, McGraw-Hill, New York, (2002) 2.185.

[6] A. Ramanathan, M. S. Hamdy, R. Parton, T. Maschmeyer, J. C. Jansen, U. Hanefeld, Appl. Catal. A: Gen. 355 (2009) 78-82.

[7] D. Alberico, M. E. Scott, M. Lautens, Chem. Rev. 107 (2007) 174-238.

[8] J. M. Thomas, B. F. G. Johnson, R. Raja, G. Sankar, P. A. Midgley, Acc. Chem. Res. 36 (2003) 20-39.

[9] T. F. S. Silva, T. C. O. Mac Leod, L. M. D. R. S. Martins, M. F. C. G. da Silva, M. A. Schiavon, A. J. L. Pombeiro, J. Mol. Catal. A: Chem. 367 (2013) 52-60.

[10] H. Hattori, Y. Ide, S. Ogo, K. Inumaru, M. Sadakane, T. Sano, ACS Catal. 2 (2012) 1910-1915.

[11] H. X. Yuan, Q. H. Xia, H. J. Zhan, X. H. Lu, K. X. Su, Appl. Catal. A: Gen., 304 (2006) 178-184.

[12] M. Conte, X. Liu, D. M. Murphy, K. Whiston, G. J. Hutchings, Phys. Chem. Chem. Phys. 2012, **14**, 16279-16285.

[13] J. Gu, Y. Huang, S. P. Elangovan, Y. Li, W. Zhao, I. Toshio, Y. Yamazaki, J. Shi, J. Phys. Chem. C 115 (2011) 21211- 21217.

[14] M. P. de Almeida, L. M. D. R. S. Martins, S. A. C. Carabineiro, T. Lauterbach, F. Rominger, A. S. K. Hashmi, A. J. L. Pombeiro, J. L. Figueiredo, Catal. Sci. Technol. 3 (2013) 3056-3069.

[15] C. H. Wang, L. F. Chen, Z. W. Qi, Catal. Sci. Technol. 3 (2013) 1123-1128.

[16] R. Zhao, Y. Wang, Y. Guo, Y. Guo, X. Liu, Z. Zhang, Y. Wang, W. Zhan, G. Lu, Green Chem. 8 (2006) 459-466.

[17] H. Wang, R. Li, Y. Zheng, H. Chen, F. Wang, J. Ma, Catal. Lett. 122 (2008) 330-337.

[18] Y. Shiraishi, Y. Sugano, S. Ichikawa, T. Hirai, Catal. Sci. Technol. 2 (2012) 400-405.

[19] B. Sarkar, P. Prajapati, R. Tiwari, R. Tiwari, S. Ghosh, S. S. Acharyya, C. Pendem, R. K. Singha, L. N. Sivakumar Konathala, J. Kumar, T. Sasaki, R. Bal, Green Chem. 14 (2012) 2600-2606.

[20] S. Samanta, N. K. Mal, A. Bhaumik, J. Mol. Catal. A: Chem. 236 (2007) 7-11.

[21] N. K. Mal, A. Bhaumik, R. Kumar, A.V. Ramaswamy, Catal. Lett. 33 (1995) 387-394.

[22] A. Tabler, A. Haeusser, E. Roduner, J. Mol. Catal. A: Chem. 379 (2013) 139-145.

[23] R. Kumar, P. Mukherjee, A. Bhaumik, Catal. Today 49 (1999) 185-191.

[24] M. E. Lydon, K. A. Unocic, T. H. Bae, C. W. Jones, S. Nair, J. Phys. Chem. C 116 (2012) 9636-9645.

(2012) 9636-9645.

[25] S. E. Dapurkar, A. Sakthivel, P. Selvam, J. Mol. Catal. A: Chem. 223 (2004) 241-250.

[26] T. Sen, P. R. Rajamohanan, S. Ganapathy, S. Sivasanker, J. Catal. 163 (1996) 354-364.

[27] W. Wang, G. Ding, T. Jiang, P. Zhang, T. Wu, B. Han, Green Chem. 2013, **15**, 1150-1154.

[28] M. -J.; Cheng, W. A. Goddard, J. Am. Chem. Soc. 2013, **135**, 4600-4603.

[29] C. Martínez, A. Corma, Coord. Chem. Rev. 255 (2011) 1558-1580.

[30] H. Y. Lue, L. Bui, W. R. Gunther, E. Min, Y. Román-Leshkov, ACS Catal. 2 (2012) 2695-2699.

[31] Y. Huang, K. Wang, D. H. Dong, D. Li, M. R. Hill, A. J. Hill, H. Wang, Micropor. Mesopor. Mater. 127 (2010) 167-176.

[32] A. H. Ahmed, J. Appl. Sci. Res. 3 (2007) 1663-1670.

[33] M. M. Najafpour, B. Pashaei, Dalton Trans. 41 (2012) 10156-10160.

[34] V. Rama, K. Kanagaraj, T. Subramanian, P. Suresh, K. Pitchumani, Catal. Commun. 26 (2012) 39-43.

[35] K. O. Xavier, J. Chacko, K. K. M. Yusuff, Appl. Catal. A: Gen. 258 (2004) 251-259.

[36] H. S. Abbo, S. J. J. Titinchi, Appl. Catal. A: Gen. 356 (2009) 167-171.

[37] L. Agasi, F. J. Berry, M. Carbucicchio, J. F. Marco, M. Mortimer, F. F. F. Vetel, J. Mater. Chem. 12 (2002) 3034-3038.

[38] M. Wark, M. Koch**,** A. Brückner, W. Grünert**,** J. Chem. Soc., Faraday Trans. 94 (1998) 2033-2041

2033-2041.

[39] Y. Okamoto, M. Ogawa, A. Maezawa, T. Imanaka, J. Catal. 112 (1988) 427-436.

[40] S.-B. Kim, K.-W. Lee, Y.-J. Kim, S.-I. Hong, Bull. Korean Chem. Soc. 1994, **15**, 424-427.

[41] O.-S. Park, S.-S. Nam, S.-B. Kim, K.-W. Lee, Bull. Korean Chem. Soc. 20 (1999) 49-52.

[42] J. Hartung, Pure Appl. Chem. 77 (2005) 1559-1574.

[43] S. K. Maiti, S. Dinda, M. Nandi, A. Bhaumik, R. G. Bhattacharyya, J. Mol. Catal. A: Chem. 287 (2008) 135-141.

[44] J. Li, Y. Shi, L. Xu, G. Lu, Ind. Eng. Chem. Res. 49 (2010) 5392-5399.

[45] T. Tatsumi, Y. Watanabe, Y. Hirasawa, J. Tsuchiya, Res. Chem. Intermed. 24 (1998) 529-540.

[46] P. Borah, A. Datta, Appl. Catal. A: Gen. 376 (2010) 19-24

[47] W. A. Carvalho, P. B. Varaldo, M. Wallau, U. Schuchardt, Zeolites 18 (1997) 408-416.

[48] M. Nowotny, L. N. Pedersen, U. Hanefeld, T. Maschmeyer, Chem. Eur. J. 8 (2002) 3724-3731.

[49] C. Nguyen, R. J. Guajardo, P. K. Mascharak, Inorg. Chem. 35 (1996) 6273-6281.

[50] A. Corma, Chem. Rev. 97 (1997) 2373-2419.

[51] J. Hájek, N. Kumar, P. Mäki-Arvela, T. Salmi, D. Yu. Murzin, I. Paseka, T. Heikkilä, E. Laine, P. Laukkanen, J. Väyrynen, Appl. Catal. A: Gen. 251 (2003) 385-396.

**Legend for Figures**

**Figure 1.** Powder XRD patterns of (a) Na-Y and (b) V-Y samples. Vertical lines indicate the peak positions in both the samples.

**Figure 2.** A: $N_2$ adsorption (●)-desorption (○) isotherms of the parent zeolite Na-Y (a) and V-Y (b) material. For clarity, Y-axis points of V-Y sorption have been 130. B: Adsorbed $N_2$ gas volume Vs statistical thickness of pores in the material.

**Figure 3.** A: TEM image of the sample V-Y and B: TEM image of the sample showing reflection planes.

**Figure 4.** EDS elemental mapping of V-Y sample. a: O, b: Al, c: Si and d: V elements, respectively. e: the whole EDX spectrum of the sample V-Y.

**Figure 5.** FT IR data of (a) Na-Y, (b) the catalyst V-Y and (c) the recovered catalyst V-YR. (*) indicates the peak for $CO_2$.

**Figure 6.** X-ray photoelectron spectra of A: V 2p, B: Si 2p, C: Al 2p and D: O 1s core level electrons of V-Y.

**Figure 7.** A: Effect of reaction time and B: the amount of TBHP on the % yield of cyclohexanone over V-Y catalyst.

**Figure 8.** Recycling efficiency of V-Y in one pot oxidation of cyclohexane to cyclohexanone. For convenience all cycles are continued for 24 h only.

**Table 1.** Physico-chemical data of the catalyst V-Y.

| Sample name | $S_{BET}$ [$m^2g^{-1}$] | $S_{micro}$ [$m^2g^{-1}$] | $S_{ext}$ [$m^2g^{-1}$] | $D_p$ [nm] | $V_t$ [$cm^3g^{-1}$] | $V_{micro}$ [$cm^3g^{-1}$] | Presence of V (%)[1] |
|---|---|---|---|---|---|---|---|
| Na-Y | 686 | 672 | 14.4 | 2.25 | 0.34 | 0.32 | - |
| V-Y | 139.4 | 135.0 | 3.80 | 2.59 | 0.063 | 0.060 | 15.10 |

$S_{BET}$ = BET surface area, $S_{micro}$ = micropore surface area, $S_{micro}$ = external surface area, $D_p$ = average pore diameter corresponding to the maximum of PSD curve, $V_t$ = total pore volume, $V_{micro}$ = micropore volume.

[1]Estimated through AAS analysis.

**Table 2.** Binding energies of core level electrons obtained from XPS study of V-Y zeolite (with refernece to O 1s binding energy at 532.0 eV)

| Core level electron | Binding energy (eV) |
|---|---|
| V 2p | 516.51 |
| | 523.42 |
| Si 2p | 102.85 |
| Al 2p | 74.30 |
| O 1s | 532.00 |

**Table 3.** Catalytic oxidation of cyclohexane (CH) to cyclohexanone (CHone) over different catalysts.

| Entry | Catalyst | Reaction time (h) | CH conversion (%) | CHone selectivity (%) |
|---|---|---|---|---|
| 1 | V-Y | 72 | 97.76 | 100 |
| 2 | V-Y | 24 | 38.10 | 100 |
| 3 | NaY | 24 | 3.23 | - |
| 4[a] | - | 24 | 1.81 | - |
| 5[b] | V-Y | 24 | 0.00 | - |
| 6[c] | V-Y | 24 | 2.36 | 100 |
| 7[d] | V-Y | 24 | 9.65 | 100 |

Conversion (%) = [Peak area of product obtained from GC/Summation of peak area of substrate and product obtained from GC]*100.

Reaction conditions: cyclohexane = 1 mmol, TBHP = 0.75 g, catalyst = 0.05 g, room temperature,

[a] blank reaction carried out without any catalyst.

[b] reaction carried out without TBHP.

[c] reaction carried out using $H_2O_2$ instead of TBHP.

[d] reaction carried out with 1:1 mixture of $H_2O_2$ and TBHP.

**Table 4.** Comparative catalytic performance of reported oxidation catalysts with our materials.

| Entry | Catalyst | Time (h) | Temp (K) | Oxidant | Solvent | CH conversion (%) | CHone selectivity (%) | Ref. |
|---|---|---|---|---|---|---|---|---|
| 1 | V-MCM-41 | 12 | 373 | $H_2O_2$ | Acetic acid | 99.0 | 1.9 | 25 |
| 2 | V-HMS | 4 | 413 | $O_2$ | No solvent | 9.34 | 60.3 | 46 |
| 3 | VS-2 | 4 | 333 | $H_2O_2$ | Acetonitrile | 28[1] | - | 47 |
| 4 | $VOPO_4$ on alumina | 24 | 333 | $H_2O_2$ | Acetonitrile | 59.0 | 9.7 | 48 |
| 5 | V-MCM-41 | 12 | 373 | TBHP | Acetone or cyclohexane | 44.6 | 61.29 | 49 |
| 6 | V-MCM-41 | 12 | 373 | $H_2O_2$ | Acetone | 11.67 | 57.14 | 49 |
| 7 | V-Y | 72 | 303 | TBHP | No solvent | 97.76 | 100.0 | This work |

[1]TON = Turn over number, moles of cyclohexane converted per mole of V.

Figure 1 (Pal et al)

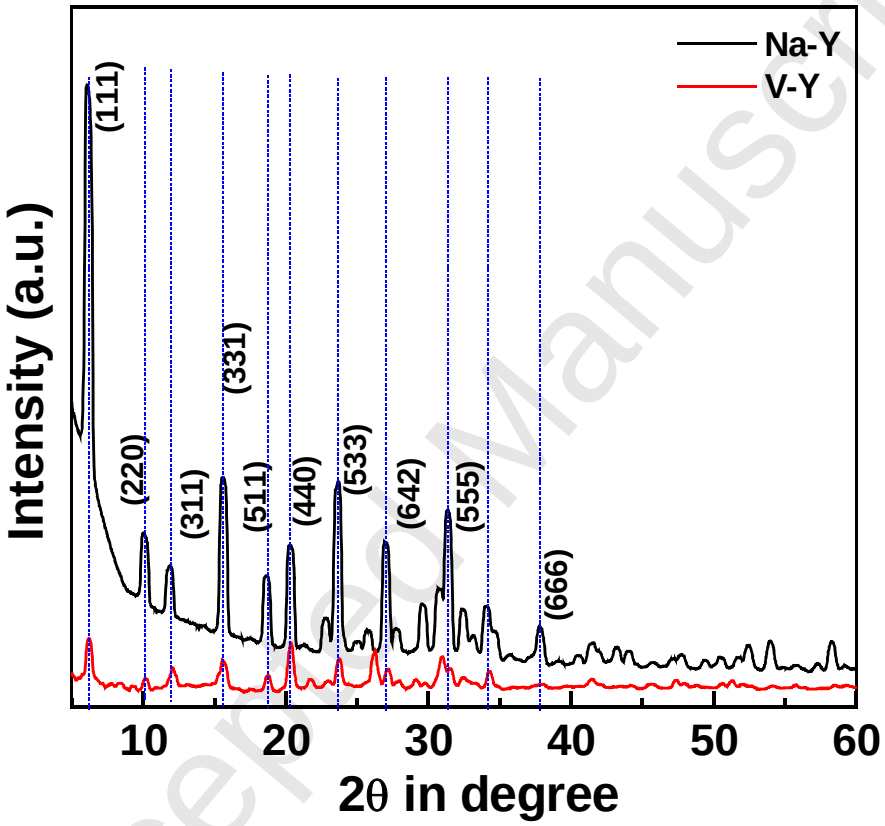

Figure 2 (Pal et al)

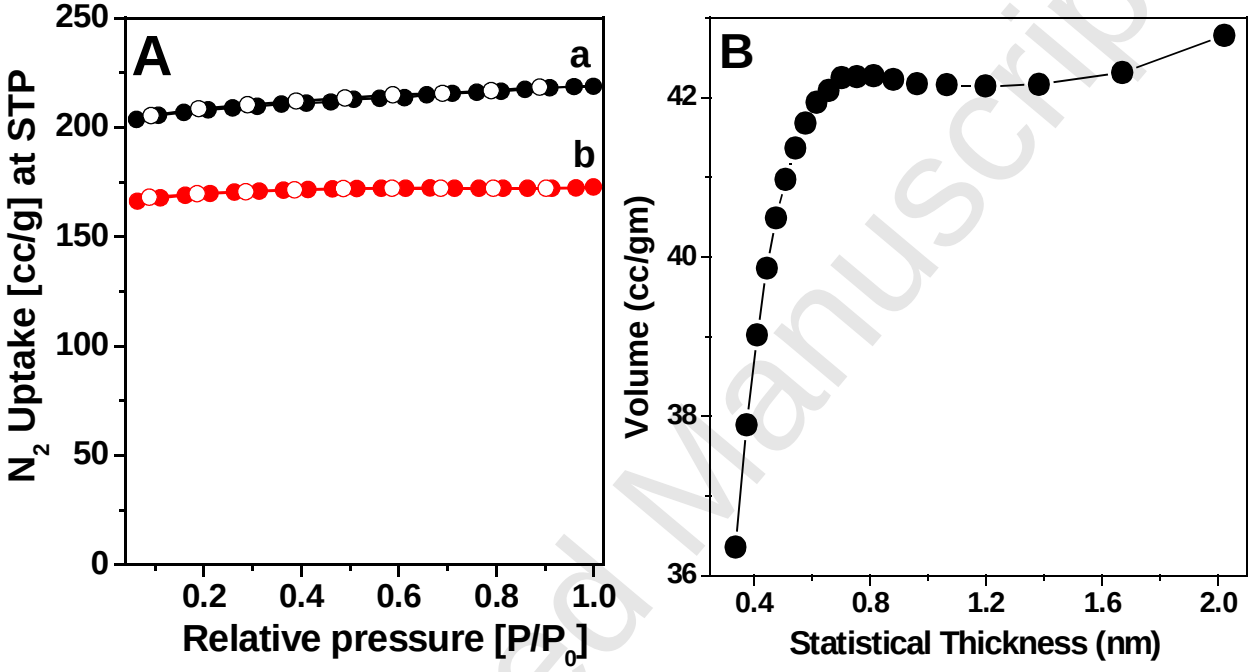

Figure 3 (Pal et al)

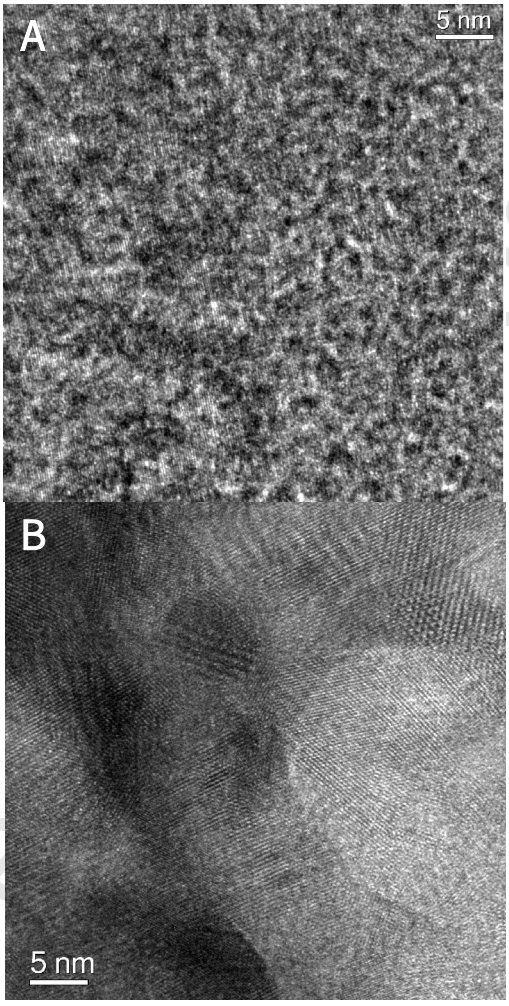

Figure 4 (Pal et al)

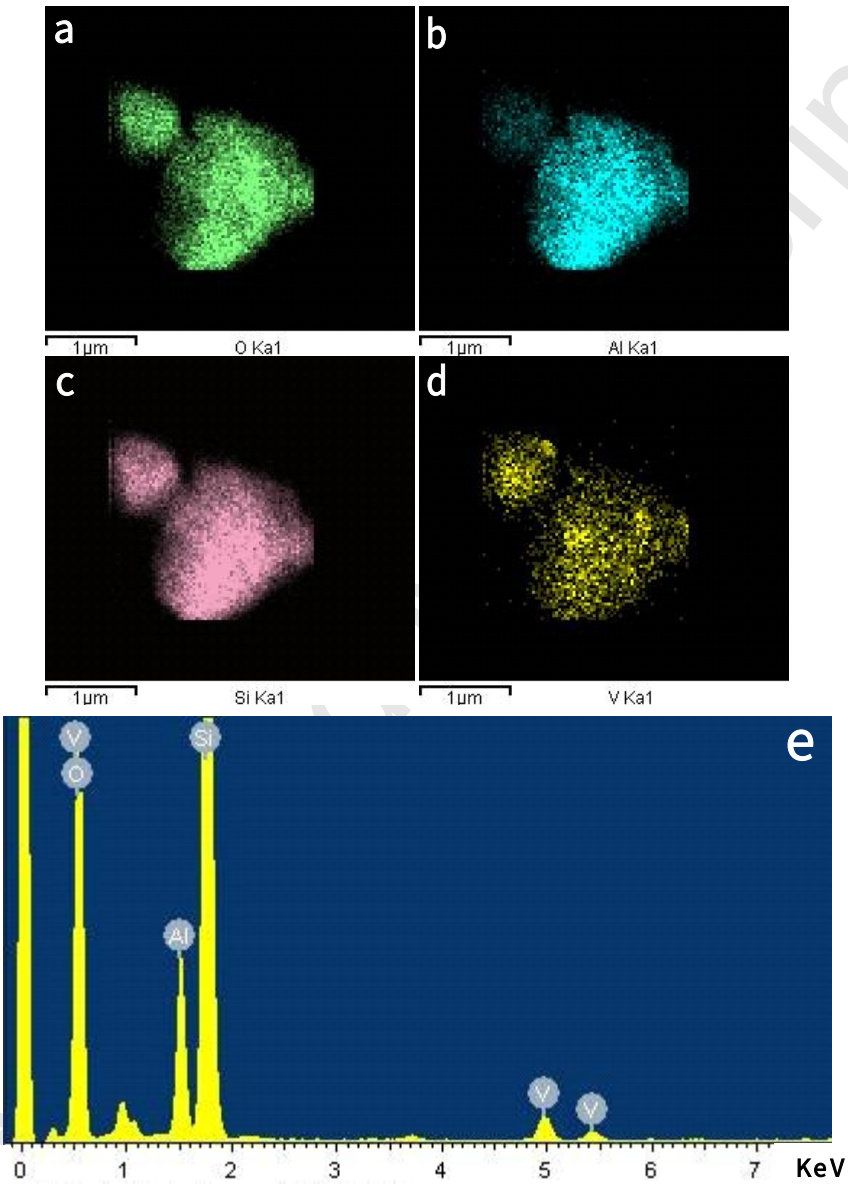

Figure 5 (Pal et al)

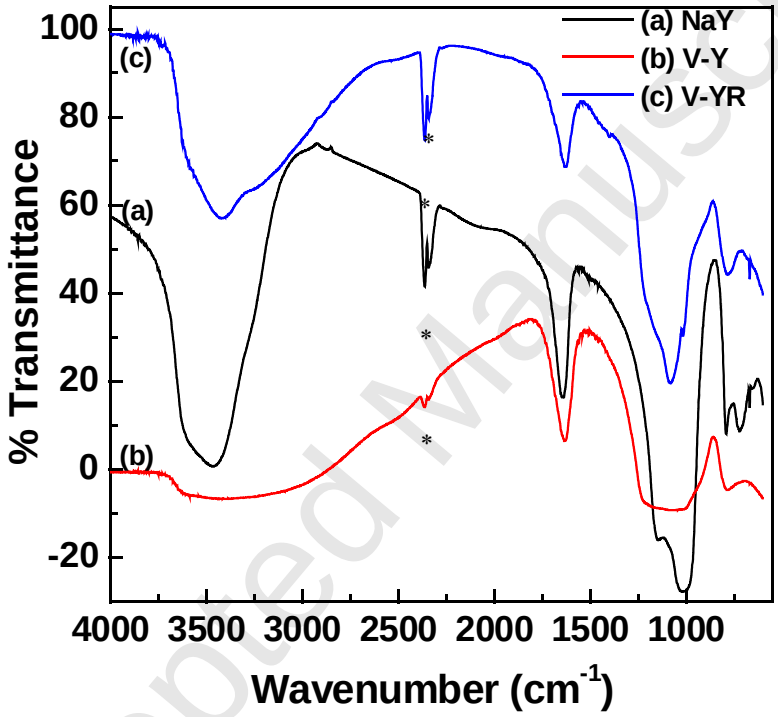

Figure 6 (Pal et al)

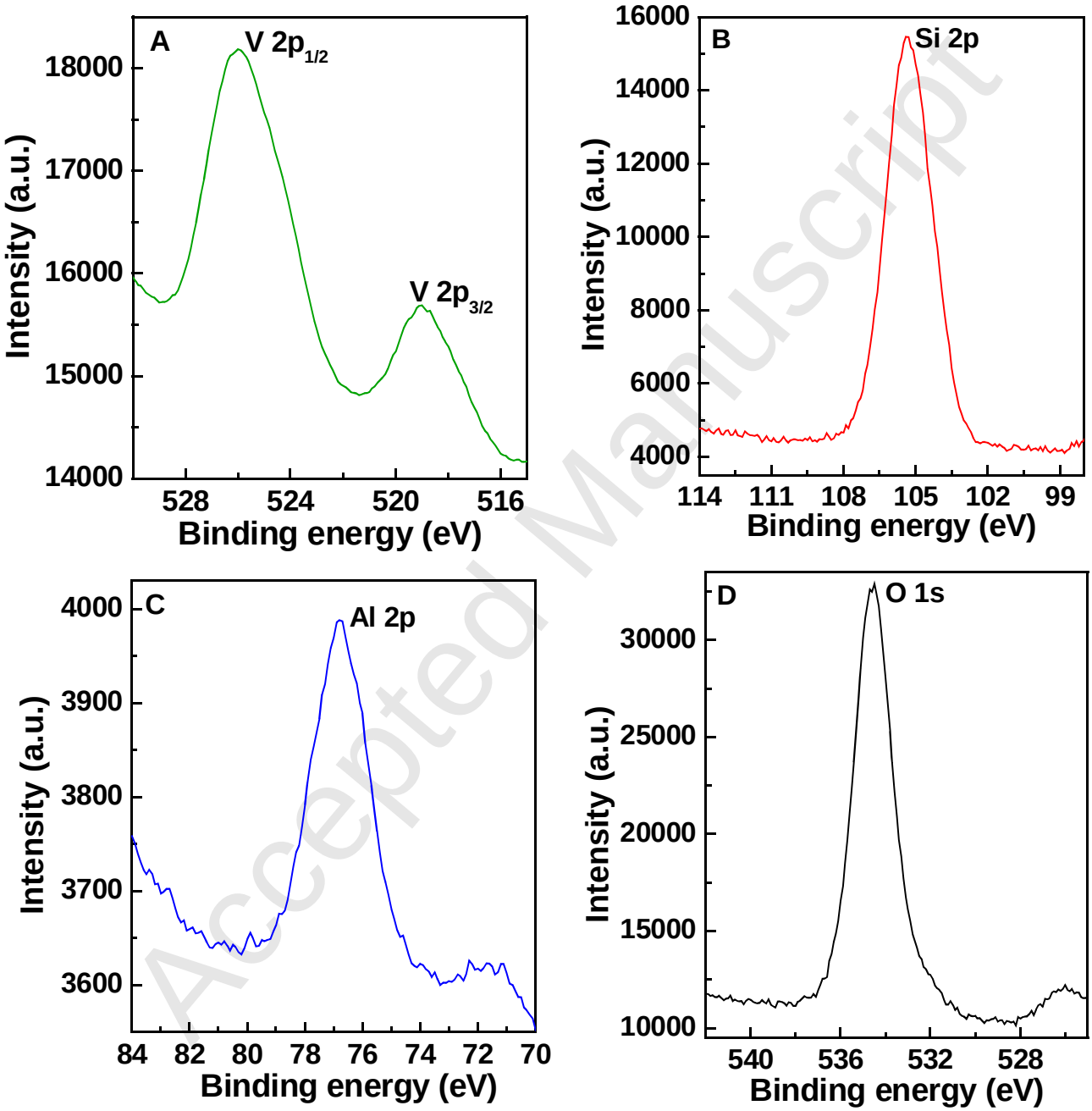

Figure 7 (Pal et al)

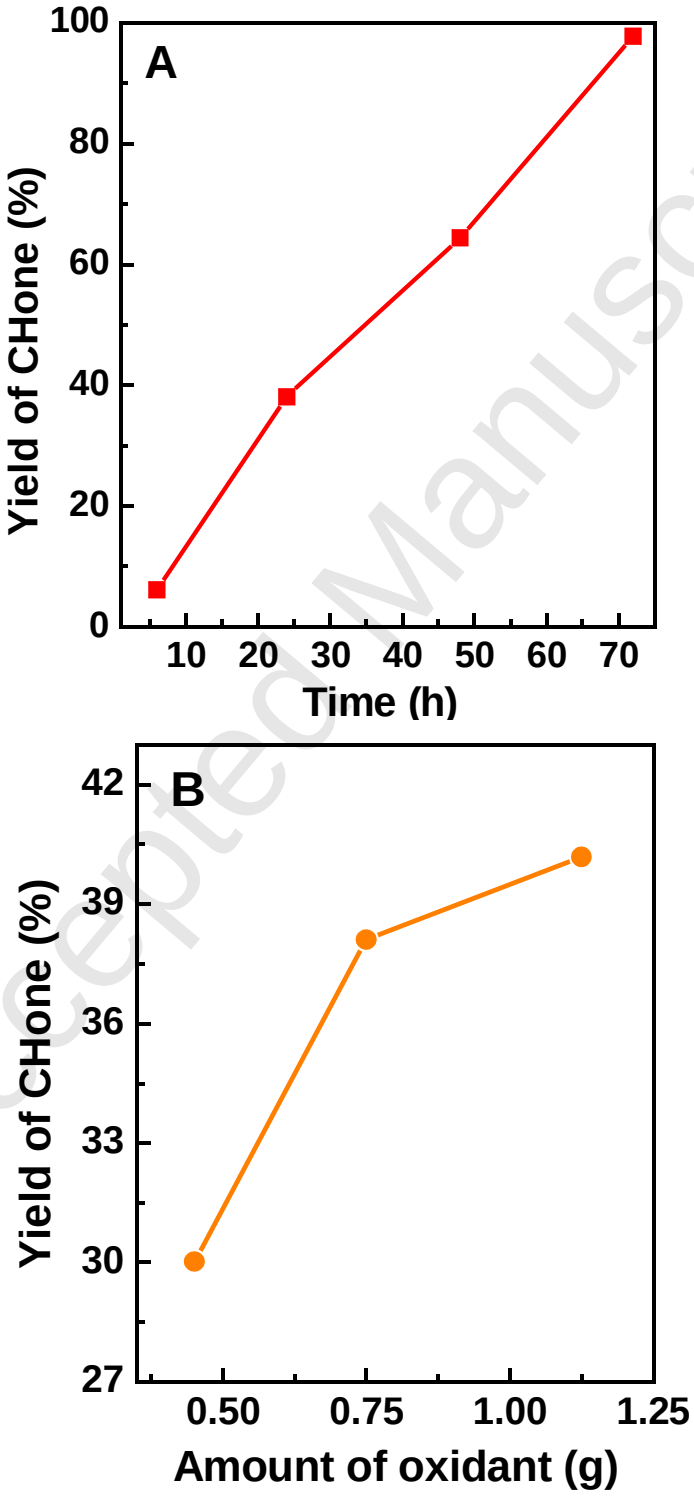

Figure 8 (Pal et al)

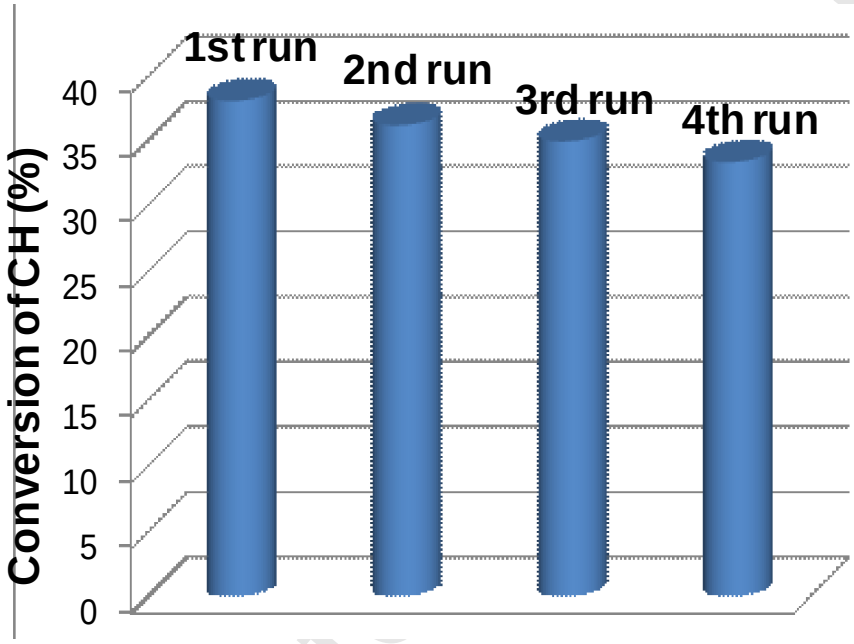

Scheme 1 (Pal et al)

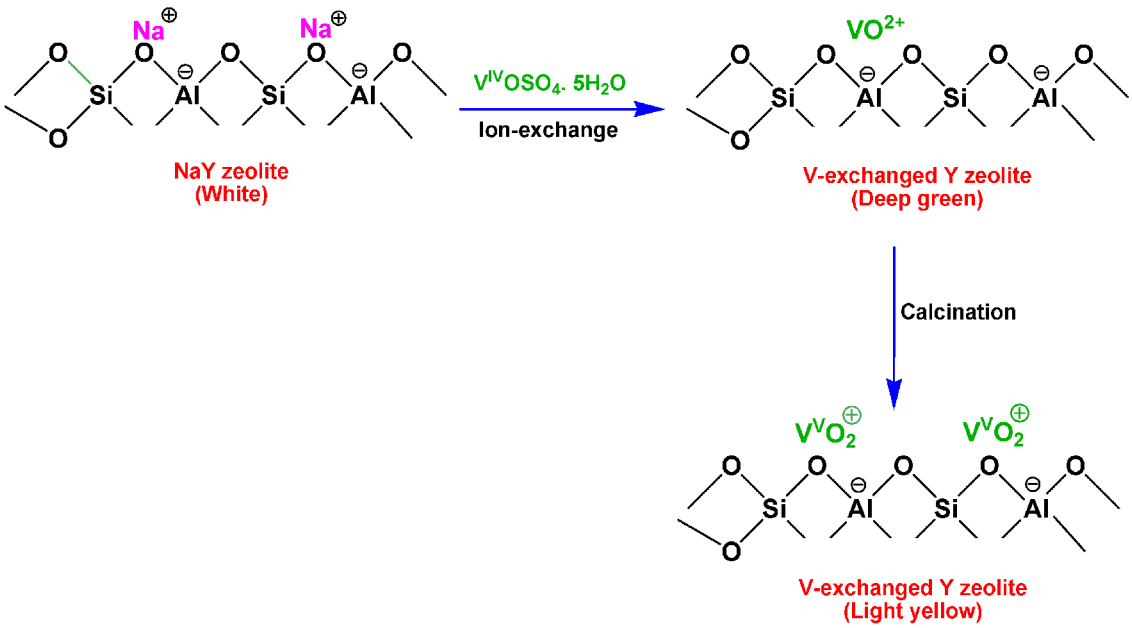


**Scheme 1:** Schematic representation depicting the formation of V-exchanged Y zeolite (V-Y).

Scheme 2 (Pal et al)

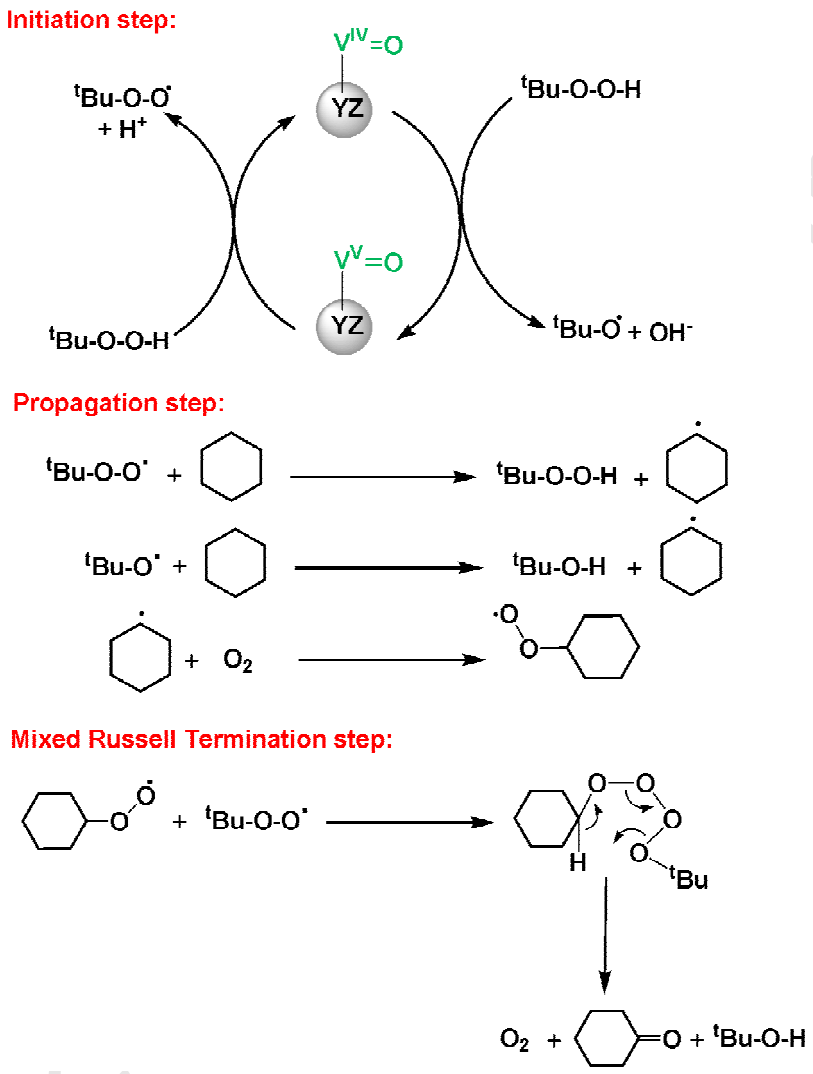


**Scheme 2:** Proposed mechanism for cyclohexane oxidation via free-radical reaction pathway over V-Y catalyst.